Inflammation, Vol. 42, No. 1, February 2019 (© 2018)
DOI: 10.1007/s10753-018-0903-7

ORIGINAL ARTICLE

IRF-1 Intervention in the Classical ROS-Dependent Release of NETs during LPS-Induced Acute Lung Injury in Mice

Shuai Liu,[1] Yinyan Yue,[2] Pinhua Pan,[1,4] Lemeng Zhang,[3] Xiaoli Su,[1] Haitao Li,[1] Haosi Li,[1] Yi Li,[1] Minhui Dai,[1] Qian Li,[1] and Zhi Mao[1]

Abstract— Previously, we demonstrated that neutrophil extracellular traps (NETs) play an essential role in lipopolysaccharide (LPS)-induced acute lung injury. However, the underlying mechanism is unclear. In this study, we showed that knockout of interferon regulatory factor 1 (IRF-1) in mice strongly attenuated the generation of NETs and reactive oxygen species (ROS) production in neutrophils from bronchoalveolar lavage fluid and alleviated LPS-induced lung injury and systemic inflammation. Our *in vitro* experiments demonstrated that LPS-stimulated platelets induce NET release through two distinct processes: an ROS-independent early/rapid NETosis and a later ROS-dependent classical NETosis. Notably, the classical ROS-dependent pathway plays a dominant role in the generation of NETs. Furthermore, we showed that IRF-1 knockout does not affect the formation of NETs in early/rapid NETosis, but significantly attenuates ROS production and the generation of NETs in classical NETosis, which determines the total levels of NETs released by LPS-stimulated platelets. In conclusion, IRF-1 deficiency plays a key role in moderating the excessive NETs formed *via* ROS in the classical pathway and retaining the protective role of the low-NET levels generated in early/rapid NETosis, which may serve as a novel target in acute lung injury/acute respiratory distress syndrome.

KEY WORDS: acute lung injury; interferon regulatory factor-1; neutrophil extracellular traps; reactive oxygen species; lipopolysaccharide.

INTRODUCTION

Acute respiratory distress syndrome (ARDS) is characterized by acute hypoxemic respiratory failure, bilateral pulmonary infiltrates, and pulmonary edema of non-cardiac origin. ARDS remains a major cause of mortality in intensive care units worldwide [1, 2]. Until recently, there was no specific or effective preventive strategy for ARDS and no suitable therapeutic options, with treatment primarily consists of supportive care. Sepsis is one of the most common etiologies of ARDS [3], and mouse models of sepsis-induced acute lung injury (ALI) are used to elucidate the pathogenesis of ARDS [4]. Lipopolysaccharide (LPS) administration is the most commonly used approach to model the consequences of bacterial sepsis

[1] Department of Respiratory and Critical Care Medicine (Department of Respiratory Medicine), Key cite of National Clincial Research Center for Respiratory Disease, Xiangya Hospital, Central South University, Changsha, 410008, Hunan, China
[2] Department of Pediatrics, Xiangya Hospital, Central South University, Changsha, 410008, Hunan, China
[3] Department of Thoracic Medicine, Hunan Cancer Hospital, Affiliated to Xiangya Medical School, Central South University, Changsha, 410013, Hunan, China
[4] To whom correspondence should be addressed at Department of Respiratory and Critical Care Medicine (Department of Respiratory Medicine), Key cite of National Clincial Research Center for Respiratory Disease, Xiangya Hospital, Central South University, Changsha, 410008, Hunan, China. E-mail: pinhuapan668@126.com

[5], and our study predominantly focuses on sepsis-induced ALI to identify novel and effective therapeutic targets and approaches for ARDS.

Migration and accumulation of neutrophils into the alveolar space in the early inflammatory response were observed in infection-related ALI/ARDS [6]. Neutrophils are activated and lodge primarily in the capillaries of the lungs, which is believed to be a harmful effect of inappropriate neutrophil activation due to bacteremia or endotoxemia as a result of bacterial shedding of LPS [7]. The antimicrobial mechanisms of neutrophils include phagocytosis and release of antimicrobial substances *via* degranulation. Additionally, a novel antibacterial strategy that localizes and eliminates pathogens, called neutrophil extracellular traps (NETs), has been described [8]. NETs are webs of histone-modified nuclear material and proteins that include elastase and MPO extruded from activated neutrophils during the inflammatory response [8]. Activated neutrophils can release NETs to trap microorganisms from the infection site or blood and kill them. However, our recent study found that excessive NETs formed during LPS-induced ALI caused organ damage and initiated the inflammatory response [9]. Therefore, strategies to attenuate excessive NET formation or retain the physiological role of NETs may benefit patients with ARDS.

Previously, we demonstrated that platelets activated by LPS could induce NET production effectively [9], but the molecular mechanisms underlying NET formation are still poorly understood. To date, two major NET release mechanisms have been proposed: the classical reactive oxygen species (ROS)-dependent and the early/rapid ROS-independent mechanism [10, 11]. In the classical mechanism, neutrophils undergo a cell death program that culminates with the release of NETs 1 to 4 h after activation, in a process that is dependent on ROS production. However, neutrophils can release NETs without activation of the nicotinamide adenine dinucleotide phosphate (NADPH) oxidase complex. During the early/rapid vital NETosis mechanism, neutrophils extrude NETs after as little as 5 to 15 min of activation, without affecting neutrophil viability. In this study, we investigated whether ROS are involved in the NET formation induced by activated platelets in mouse neutrophils.

Interferon regulatory factor-1 (IRF-1) has been closely associated with the release of inflammatory mediators, apoptosis, and autophagy during sepsis-related organ damage [12, 13]. Our previous study found that IRF-1 was an upstream mediator of HMGB1 release in macrophages following LPS stimulation [14]. HMGB1 was reported to induce the formation of NETs by TLR4 and TLR9 receptors in a liver ischemia reperfusion injury model [15]. Furthermore, the absence of IRF-1 in genetic knockout mice strongly abrogated the observed effects of TNF-α/IFN-γ on ROS production and loss of mitochondrial transmembrane potential ($\Delta\Psi$m) compared with IRF-1(+/+) mice [16]. Inflammatory mediators (*e.g.*, HMGB1), autophagy, and ROS production are all closely related to the formation of NETs [8, 10, 17]. Therefore, we hypothesized that IRF-1 regulates the formation of NETs through ROS.

In the present study, we demonstrated that the absence of IRF-1 in genetic knockout mice strongly alleviates LPS-induced lung injury and decreases NET release. The data also suggest that IRF-1 does not regulate the early/rapid ROS-independent NETosis but does play a key role in controlling the classical ROS-dependent NETosis mechanism, which is the leading cause of NET generation and can determine the level of NETs in experimental ALI. Our study provides a novel perspective on the pathogenesis of ALI/ARDS.

MATERIALS AND METHODS

Major Reagents

LPS (*E. coli* 0111:B4), diphenyleneiodonium (DPI), N-acetyl-L-cysteine (NAC), dihydrorhodamine 123 (DHR 123), and phorbol 12-myristate 13-acetate (PMA) were purchased from Sigma Chemical Company (St. Louis, MO, USA). Deoxyribonuclease I (DNase I) was purchased from Roche Diagnostics (Mannheim, Germany). Rabbit polyclonal IRF-1, histone H3, and β-tubulin antibodies were all from Cell Signaling Technology (Boston, MA, USA). Goat polyclonal neutrophil elastase (NE) antibody was obtained from Santa Cruz Biotechnology (Santa Cruz, CA, USA). Rabbit polyclonal Cit-H3 primary antibody and anti-rabbit Alexa 488 and anti-goat Alexa 647 secondary antibodies were obtained from Abcam (Cambridge, UK).

Mouse Experiments

Mouse experiments were approved by the Animal Care and Use Committee of the Central South University and were consistent with recommendations of the guidelines provided by the National Institutes of Health (Bethesda, MD, USA). Pathogen-free 8- to 12-week-old male IRF-1 knockout (KO) mice (Jackson Laboratory, Bar Harbor, ME, USA) and C57BL/6 mice (Experimental Animal Center of Central South University, Changsha, China) were

given intraperitoneal (IP) injections of LPS (5 mg/kg) to induce endotoxemia as described previously [18]. In some experiments, mice were treated intravenously with 2000 U DNase I in 50 μL PBS at 0 and 10 h post-injection to disrupt NET backbones; control mice received 50 μL PBS intravenously as described.

To evaluate the involvement of ROS in LPS-induced NET release, animals were intraperitoneally pretreated with the ROS scavenger NAC (150 mg/kg) 30 min before LPS injection and with the NADPH oxidase inhibitor DPI (1 mg/kg) 60 min before LPS injection [19, 20].

Sixteen hours following PBS or LPS administration, the animals were euthanized and killed. Lung and bronchoalveolar lavage fluid (BALF) was collected for further study as described previously. Briefly, the wet weight (*W*) of the left upper lung lobe was measured using an electronic scale, followed by desiccation in an oven at 65 °C for 48 h to determine the dry weight (*D*). The water content was obtained by calculating the *W*/*D* weight ratio. The remaining portions of the left lung were removed and fixed in 4% paraformaldehyde (PFA) for 24 h. The right lung was snap frozen and stored at − 80 °C for subsequent protein extraction. Lungs were lavaged with 1.0 mL of cold PBS-EDTA (0.5 M) each time through a 20-gauge catheter into the trachea and lavaged > 10 times by slowly withdrawing more than 0.8 mL lavage fluid each time. A total of 10 mL bronchoalveolar lavage (BAL) was withdrawn from each mouse. The 10 mL lavage fluid was centrifuged at 300×*g* for 10 min to pellet neutrophils. Another 2 mL of BALF was harvested immediately following sacrifice from other mice to detect total protein and cytokine levels in the BALF. Cytokine (IL-6, TNF-α, and HMGB1) concentrations from 2 mL BALF and plasma were detected using relevant ELISA kits.

Histological Assessment

Formalin-fixed paraffin-embedded lung tissue was cut into sections of 4 μm thickness and stained with hematoxylin-eosin. Histopathological changes were viewed with a light photomicroscope and were evaluated for pathological changes using a double-blind method. The severity of lung injury was evaluated using a semiquantitative histological index, as described previously [21]. The histological index of lung damage included alveolar edema, hemorrhage, alveolar septal thickening, and infiltration of polymorphonuclear leukocytes. Each item was divided into four grades from 0 to 3 (0 = normal, 1 = mild, 2 = moderate, 3 = severe) and then calculated for a total ALI score [21].

Isolation of Neutrophils and Platelets

Mouse neutrophils from bone marrow or BALF and platelets from anticoagulated blood were isolated and processed as described previously [9]. Briefly, for neutrophil isolation from mouse bone marrow or BALF, a commercially available mouse Neutrophil Isolation Kit (Miltenyi Biotec, Germany) was used. The purity of the neutrophil preparations (consistently > 95%) was then verified with Giemsa staining, and cell viability (> 97%) was verified by Trypan blue exclusion assay.

For platelet preparation, citrate-anticoagulated whole blood was centrifuged at 160 g for 10 min, and the platelet-rich plasma was collected and subsequently filtered through a Sepharose 2B column equilibrated with 25 mM piperazine diethanesulfonic acid buffer (PIPES). The platelets were then centrifuged at 650 g for 10 min, and the precipitate was collected and resuspended in RPMI 1640.

Identification of NETs *In Vivo* and *In Vitro*

Paraffin-embedded mouse lungs were sectioned (4 μm), and sections were prepared and mounted on glass slides. After dewaxing and antigen retrieval with citrate buffer, specimens were blocked with PBS containing 5% BSA. Sections were incubated with the primary antibodies anti-citrullinated histone H3 (1:100) and anti-neutrophil elastase (1:50), followed by detection with Alexa Fluor 488 donkey anti-rabbit (1:500) and Alexa Fluor 647 donkey anti-goat (1:500) secondary antibodies overnight at 4 °C, respectively. Then, 4′, 6-diamidino-2-phenylindole (DAPI) was used for DNA detection.

For the *in vitro* experiments, neutrophils (5×10^5) were plated to adhere in coated plates for 1 h before stimulation for 10 min or 90 min with phorbol 12-myristate 13-acetate (PMA, 100 nM), LPS (1 μg/ml), platelets (5×10^6), and LPS with platelets. The samples were fixed with 4% paraformaldehyde and blocked with 5% bovine serum albumin (BSA) for 1 h at room temperature. Slides were incubated with the primary or secondary antibodies mentioned above at concentrations of 1:600, 1:100, 1:800, and 1:800, respectively. Slides were visualized with an Olympus FluoView500 confocal microscope.

Quantification of NETs

To quantify NET release in BALF and cell culture supernatant, MPO-DNA complex levels were measured as previously described [22]. In brief, NET-associated MPO was captured using a mouse MPO ELISA kit (Hycult Biotech, HK210–01), after which a peroxidase-labeled

anti-DNA monoclonal antibody (component 2, Cell Death ELISA^{PLUS}, Roche; Cat. No: 11774424001) was used to detect the NET-associated DNA backbone. NET release values are depicted as the fold increase compared with controls.

Cellular and Nuclear Protein Extraction

The collected cells were centrifuged at 500 g for 3 min. These pellets were then resuspended with cytoplasmic extraction reagent (Vazyme, China) on ice, combined with protease inhibitor mix for 10 min, and centrifuged at 16,000 g for 5 min at 4 °C to extract total cellular protein. For nuclear protein isolation, the cell pellet was lysed with nuclear extraction reagent (Nanjing, Vazyme, China) combined with a protease inhibitor mix. Protein concentration was determined by the BCA method, and 50 μg of protein per sample was mixed with sample loading buffer and boiled for 8 min.

Western Blot

Protein samples were electrophoresed in 6 to 12% sodium dodecyl sulfate-polyacrylamide (SDS-PAGE) gels and transferred onto polyvinylidene fluoride (PVDF) membranes (Bio-Rad Laboratories, Berkeley, CA). After the membranes were blocked with 5% nonfat milk in TBS-T for 1 h at room temperature, they were incubated overnight at 4 °C with primary antibodies against citrullinated histone H3 (1:1000), IRF-1 (1:1000), histone H3 (1:500), and β-tubulin (1:1000). After three washes, membranes were incubated with the secondary antibody conjugated with horseradish peroxidase at room temperature for 1 h. The blots were developed with Super Signal chemiluminescent substrate (Pierce Chemical Co., Rockford, IL) and exposed to film. The relative quantities of the proteins were determined with a densitometer and expressed in absorbance units (AU).

Quantitative Real-Time PCR

Quantitative real-time RT-PCR analyses were performed as described previously [18]. Briefly, total RNA was extracted from neutrophils using TRIzol reagent (Invitrogen, Carlsbad, CA, USA). Then, the reverse transcript (cDNA) was synthesized using the All-in-One First-strand cDNA synthesis kit (GeneCopoeia). Finally, quantitative real-time PCR was carried out using All-in-One qPCR mix from GeneCopoeia. IRF-1 and GAPDH were used as the target and reference gene, respectively.

ROS Generation Assay

In our *in vivo* experiments, neutrophils (5×10^5, 200 μL) in BALF from wild-type (WT) and IRF-1 knockout (KO) mice were incubated with DHR123 for 30 min at 37 °C under 5% CO_2. Similarly, in our *in vitro* experiments, neutrophils (5×10^5, 200 μL) from bone marrow were preincubated with or without NAC (10 mM) or DPI (10 μM) for 30 min at 37 °C in 5% CO_2. Subsequently, 2 μM DHR123 was added and neutrophils were stimulated with LPS (1 μg/ml), platelets (5×10^6), LPS with platelets, or PMA (100 nM) for 10 min or 90 min at 37 °C, 5% CO_2. The fluorescence intensity of individual cells was analyzed with a FACSCalibur flow cytometer. Data analyses were performed with Summit v4.3 software.

Quantification of Inflammatory Indicators

IL-6, TNF-α, and HMGB1 levels in mouse plasma and BALF were determined using a commercially available mouse IL-6, TNF-α, and HMGB1 enzyme-linked immunosorbent assay (ELISA) kit (RayBiotech, USA) according to the manufacturer's instructions.

Statistical Analysis

Results are expressed as the mean ± standard deviation (SD). Differences between more than two sets of data were assessed with one-way ANOVA followed by Tukey's multiple-comparisons test. A value of $P < 0.05$ (two tailed) was considered statistically significant.

RESULTS

LPS Induces ROS-Dependent Release of NETs and IRF-1 Expression in Alveolar Neutrophils

NET formation was previously observed in LPS-induced ALI in mice [9]. In the present study, western blot analysis showed that the protein levels of citrullinated histone H3, a specific marker of NET formation, increased after LPS administration compared to PBS injection in mice (Fig. 1a, b). We measured the levels of MPO-DNA complexes in BALF and found they were significantly higher after ALI compared to the PBS injection groups (Fig. 1c).

Next, we investigated the role of ROS generation for NET formation in LPS-induced acute lung injury in mice. The ROS requirement for NET formation depends on the stimulus, as many studies have reported that ROS generation is essential for NET release, while others have shown

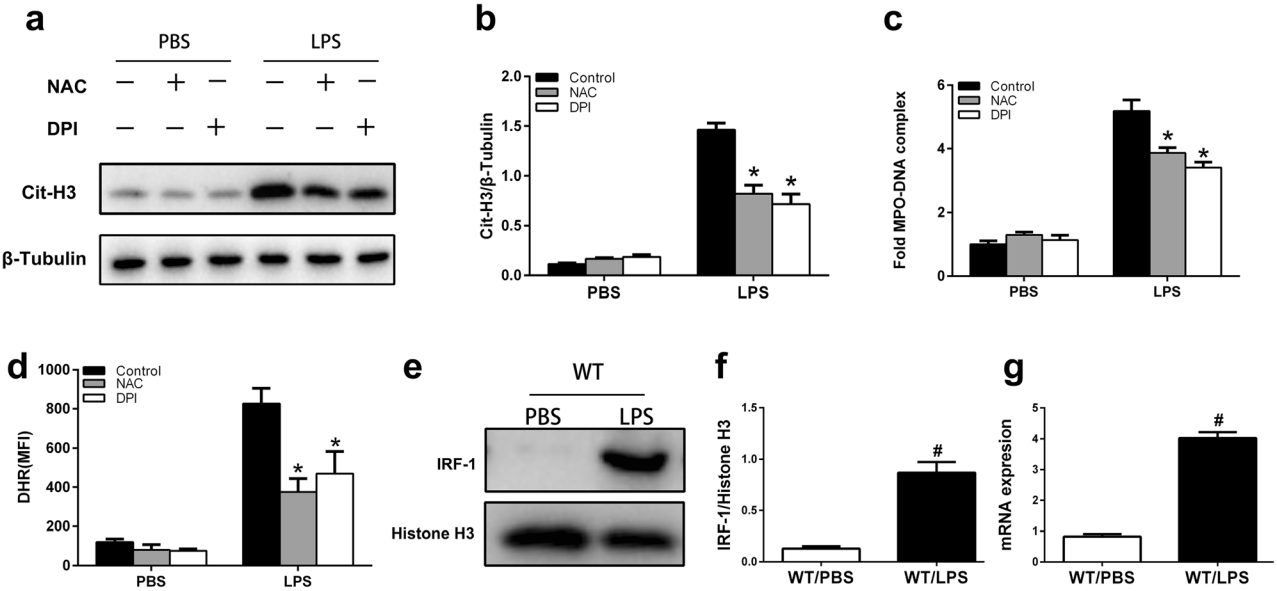

Fig. 1. LPS induces ROS-dependent release of NETs and IRF-1 expression in alveolar neutrophils. WT mice were pretreated with NAC ip (150 mg/kg) for 30 min or DPI (1 mg/kg) for 60 min before LPS administration (5 mg/kg), and lung and BALF were collected at 16 h post-treatment. **a**, **b** Cit-H3 protein levels were determined by western blot analysis in mouse lung sections. **c** Quantification of NET-associated MPO-DNA complexes. **d** After isolation, neutrophils (5×10^5) in BALF were incubated with DHR 123 for 30 min, and the MFI of individual cells was immediately analyzed by flow cytometry. **e**, **f** The expression of IRF-1 in neutrophils of BALF was determined by western blot analysis. **g** Analysis of IRF-1 gene expression in neutrophils of BALF. (n = 6/group, $^*P < 0.05$ *vs.* the control/LPS group; $^{\#}P < 0.05$ *vs.* the WT/PBS group). All data shown are representative of at least three separate independent experiments. *IRF-1* interferon regulatory factor 1; *KO* knockout; *WT* wild type; *NAC* N-acetyl-L-cysteine; *DPI* diphenyleneiodonium; *LPS* lipopolysaccharide; *PBS* phosphate-buffered saline; *BALF* bronchoalveolar lavage fluid; *Cit-H3* citrullinated histone H3; *DHR123* dihydrorhodamine 123; *MFI* mean fluorescence intensity.

them to be dispensable [10, 23]. Pretreatment with the ROS scavenger NAC inhibited LPS-induced formation of NETs in mice. Similarly, pretreatment with the NADPH oxidase inhibitor DPI also decreased LPS-induced NET production (Fig. 1a–c), indicating that ROS are necessary for NET formation by LPS.

Then, we characterized the generation of ROS specifically by neutrophils recruited to BALF after LPS administration in mice. After neutrophils of BALF were isolated, we incubated them with a fluorescent ROS probe (DHR123) and measured their mean fluorescence intensity (MFI) by flow cytometry. Our data showed that LPS induced ROS production by neutrophils in the BALF of mice. Interestingly, NAC and DPI impaired the increase in LPS-induced ROS formation, as evidenced by the low MFI of neutrophils in BALF (Fig. 1d). Taken together, these data indicated that ROS generation and NET release induced by LPS function are dependent processes.

In addition, we investigated the role of IRF-1 during LPS-induced ALI in mice. Western blot analysis demonstrated that the IRF-1 protein levels increased in the neutrophils from BALF in ALI mice (Fig. 1e, f). We also found that IRF-1 mRNA expression was significantly higher than that of the control group (Fig. 1g), a result that was consistent with our western blot analysis.

IRF-1 Deletion Attenuates LPS-Stimulated NET Release and ROS Production *In Vivo*

To determine whether IRF-1 could modulate NETosis *in vivo*, we used IRF-1 KO mice. We first performed immunofluorescence staining of lung sections and found that NET formation in IRF-KO mice was decreased compared with WT mice (Fig. 2a). As alternative approaches to assess the role of IRF-1 KO in LPS-induced NET formation, western blot and MPO-DNA capture ELISA assays were performed and demonstrated that NETs formation in IRF-1 KO mice was less than that of WT mice after LPS administration as indicated by the levels of citrullinated histone H3 in lung tissues (Fig. 2b) or the quantity of MPO-DNA complexes in BALF (Fig. 2c), consistent with the results of immunofluorescence staining.

Next, we tested the role of IRF-1 in LPS-induced ROS production by neutrophils in BALF of mice. We

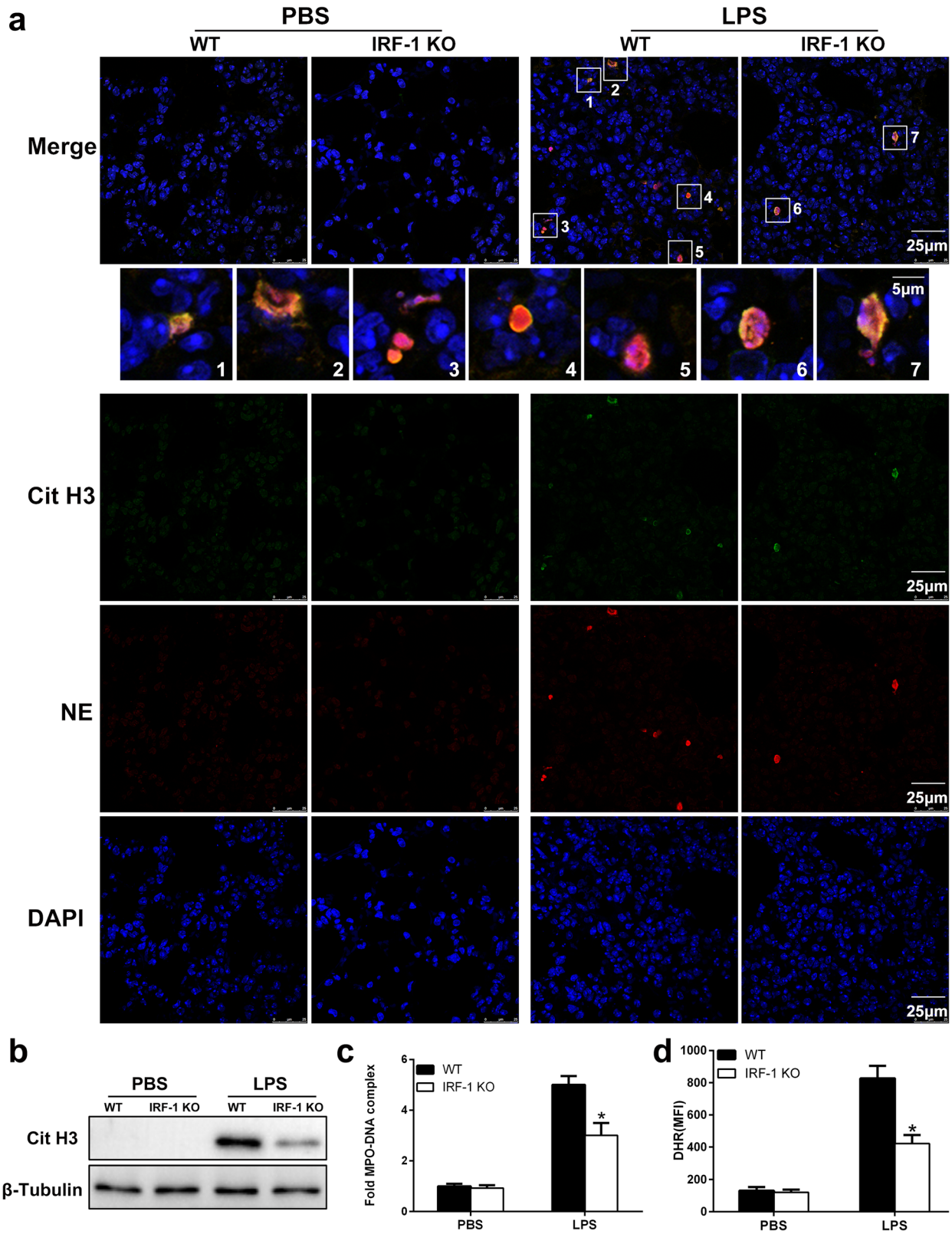
a
PBS
LPS
WT
IRF-1 KO
WT
IRF-1 KO
Merge
Cit H3
NE
DAPI
25μm
5μm
1
2
3
4
5
6
7
b
PBS
LPS
WT
IRF-1 KO
WT
IRF-1 KO
Cit H3
β-Tubulin
c
Fold MPO-DNA complex
WT
IRF-1 KO
PBS
LPS
d
DHR(MFI)
WT
IRF-1 KO
PBS
LPS

◀ **Fig. 2**. IRF-1 deletion attenuates ROS production and NET formation during LPS-induced acute lung injury in mice. WT and IRF-1 KO mice were treated with LPS or PBS for 16 h, and lung samples and BALF were collected. **a** Immunofluorescence staining of lung sections from mice was performed, with staining of Cit-H3 (green), NE (red), and DAPI (blue). The higher magnification views of the insets (1–7), which were randomly chosen, show co-localization of Cit-H3 (green), NE (red), and DNA (blue) in NET structures. **b** Cit-H3 protein levels were determined by western blot in PBS- and LPS- treated mice. **c** BALF levels of released NETs were measured by MPO-DNA capture ELISA assays. **d** The generation of ROS in neutrophils (5×10^5) of BALF, represented by MFI, was analyzed by flow cytometry. ($n = 6$ mice/group, $^*P < 0.05$ *vs.* the WT/LPS group). Results are representative of three independent experiments. *IRF-1* interferon regulatory factor 1; *KO* knockout; *WT* wild type; *LPS* lipopolysaccharide; *PBS* phosphate-buffered saline; *BALF* bronchoalveolar lavage fluid; *Cit-H3* citrullinated histone H3; *NE* neutrophil elastase; *DAPI* 4′,6-diamidino-2-phenylindole; *MFI* mean fluorescence intensity.

found that IRF-1 KO reduced ROS production compared with that in neutrophils of WT mice (Fig. 2d). Here, we demonstrated that IRF-1 KO decreased ROS production in neutrophils and NET release in the lung tissue of LPS-induced ALI; however, whether IRF-1 can regulate NET release through ROS remains unknown.

IRF-1 Deletion Attenuates LPS-Induced Acute Lung Injury and Cytokine Release in Mice

Next, we sought to investigate whether IRF-1 mediates LPS-induced acute lung injury and cytokine release. In a further set of experiments, six animal groups were created: the WT/PBS group, WT/LPS group, WT/DNase I + PBS group, WT/DNase I + LPS group, IRF-1KO/PBS group, and IRF-1KO/LPS group. Our previous results showed that treatment with DNase I was significantly protected against LPS-induced ALI and ameliorated systemic and local inflammation [9]. Similar to DNase I, IRF-1 KO also attenuated LPS-induced hemorrhaging and alveolar septal thickening compared with that of WT mice in histopathological analysis (Fig. 3a). The lung injury score (Fig. 3b), pulmonary *W/D* weight ratio (Fig. 3c), and total proteins (Fig. 3d) were significantly reduced in the IRF-1 KO/LPS group compared to the WT/LPS group, which indicated that the lung injury in IRF-1 KO mice was alleviated. Notably, however, the infiltration of neutrophils into BALF was decreased in the IRF-1 KO/LPS group compared with WT/LPS group, which was different than the results from administration of DNase I (Fig. 3e). To assess the impact of IRF-1 on systemic and local inflammatory responses, a panel of cytokines was quantified; we found that IRF-1 deletion significantly attenuated plasma and BALF levels of IL-6, TNF-α, and HMGB1 compared with the WT/LPS group, similar to the effects of DNase I administration (Fig. 4).

Involvement of ROS in Classical NETosis Triggered by LPS-Stimulated Platelets *In Vitro*

Initially, to investigate whether LPS-stimulated platelets can induce NET formation and ROS generation, we treated neutrophils with 1640 medium, platelets, LPS, LPS-stimulated platelets, and PMA for 90 min. Previously, we demonstrated that LPS (*E. coli* serotype 0111:134) alone was unable to induce NET release upon direct contact with neutrophils [9], which was consistent with other studies with neutrophils from humans or mice [17, 24–26].By measuring the levels of MPO-DNA complexes in supernatants and the MFI of DHR123-positive neutrophils, we found that LPS-stimulated platelets induced NET formation (Fig. 5a) and ROS production (Fig. 5b). Interestingly, compared with the LPS group, LPS-stimulated platelets induced higher levels of ROS production (Fig. 5b), which may be because HMGB1 present in the cell membrane of activated platelets is a potent stimulator of ROS production [27, 28]. However, after formation, NETs themselves also contributed to the accumulation of ROS in isolated neutrophils [29].

Next, we investigated whether ROS were necessary for NET release induced by LPS-stimulated platelets. Neutrophils pretreated with NAC and DPI significantly inhibited the formation of NETs (Fig. 5c). Parallel to the decrease in NETs, the generation of ROS induced by LPS-stimulated platelets was also inhibited in neutrophils of WT mice (Fig. 5d). Additionally, as an alternative method, western blot analyses obtained results consistent with those of the MPO-DNA capture ELISA assays (Fig. 5e, f). To confirm that the inhibitors used were functional and capable of blocking ROS-dependent NET formation, we performed an *in vitro* experiment showing that PMA, a well-known NET inducer, induced NET formation, and pretreatment with the inhibitors successfully blocked the formation of NETs (Fig. 5c–f). Altogether, these data indicate that classical NETosis induced by LPS-stimulated platelets was dependent on ROS.

LPS-Stimulated Platelets Activate a ROS-Independent Early/Rapid NETosis Mechanism

Leishmania and *Staphylococcus aureus* have been shown to induce early/rapid NET release through a ROS-independent pathway [11, 30]. Thus, we sought to verify whether LPS-stimulated platelets induced a similar mechanism. Indeed, LPS-stimulated platelets efficiently led to

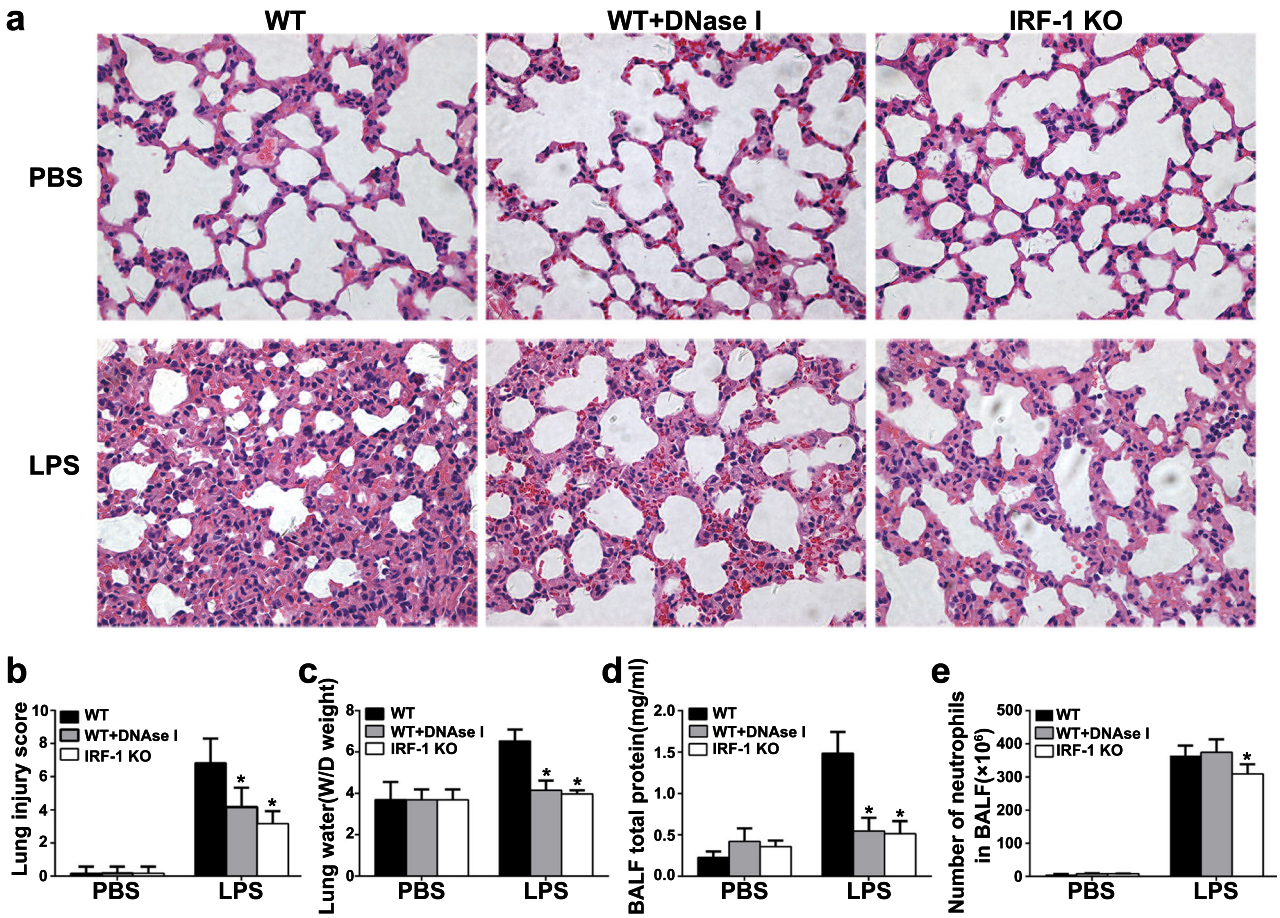

Fig. 3. IRF-1 deletion attenuates LPS-induced acute lung injury in mice. WT and IRF-1 KO mice were treated with DNase I (2000 U) at time 0 and 10 h after LPS (5 mg/kg) or PBS injection, and lung samples and BALF were collected from the mice 16 h after LPS treatment. **a** Changes in the histology of lung injury (HE, × 400); **b** the lung injury score; **c** water content of lung; **d** the total protein concentration, and **e** the number of alveolar neutrophils in BALF; ($n = 6$ mice/group, $^*P < 0.05$ *vs.* the WT/LPS group). The results are representative of three separate independent experiments. *IRF-1* interferon regulatory factor 1; *KO* knockout; *WT* wild type; *DNase I* deoxyribonuclease I; *LPS* lipopolysaccharide; *PBS* phosphate-buffered saline; *BALF* bronchoalveolar lavage fluid.

the early/rapid NET release after a 10-min incubation with neutrophils (Fig. 6a). Interestingly, in contrast to PMA, the classic NETosis inducer, LPS-stimulated platelets were unable to increase the production of ROS above control levels at this early time point (Fig. 6b, d). The data also showed that NET release in the early/rapid NETosis process was not affected by NAC or DPI, in contrast to the decrease in NET release caused by the ROS inhibitor in classical NETosis (Fig. 6c–f). In summary, these results indicate that LPS-activated platelets trigger an early/rapid NETosis independent of ROS generation.

Furthermore, we compared the contribution of the early/rapid ROS-independent and the late classical ROS-dependent NETosis to the formation of NETs. The levels of NETs released by LPS-stimulated platelets in 90 min were substantially greater than these formed in 10 min. Notably, NET formation at 90 min was significantly inhibited by NAC or DPI (Fig. 6c–f), which indicates that NET formation in the classical pathway was not solely due to the accumulation of DNA released during the early/rapid mechanism. Overall, these results showed that the classical ROS-dependent pathway plays a dominant role in the generation of NETs.

The Regulatory Role of IRF-1 in the Classical NETosis But Not in the Early/Rapid NETosis Mechanism

To investigate the kinetics of IRF-1 expression in neutrophil responses to LPS-stimulated platelets, we stimulated the neutrophils with LPS-treated platelets for 0 to

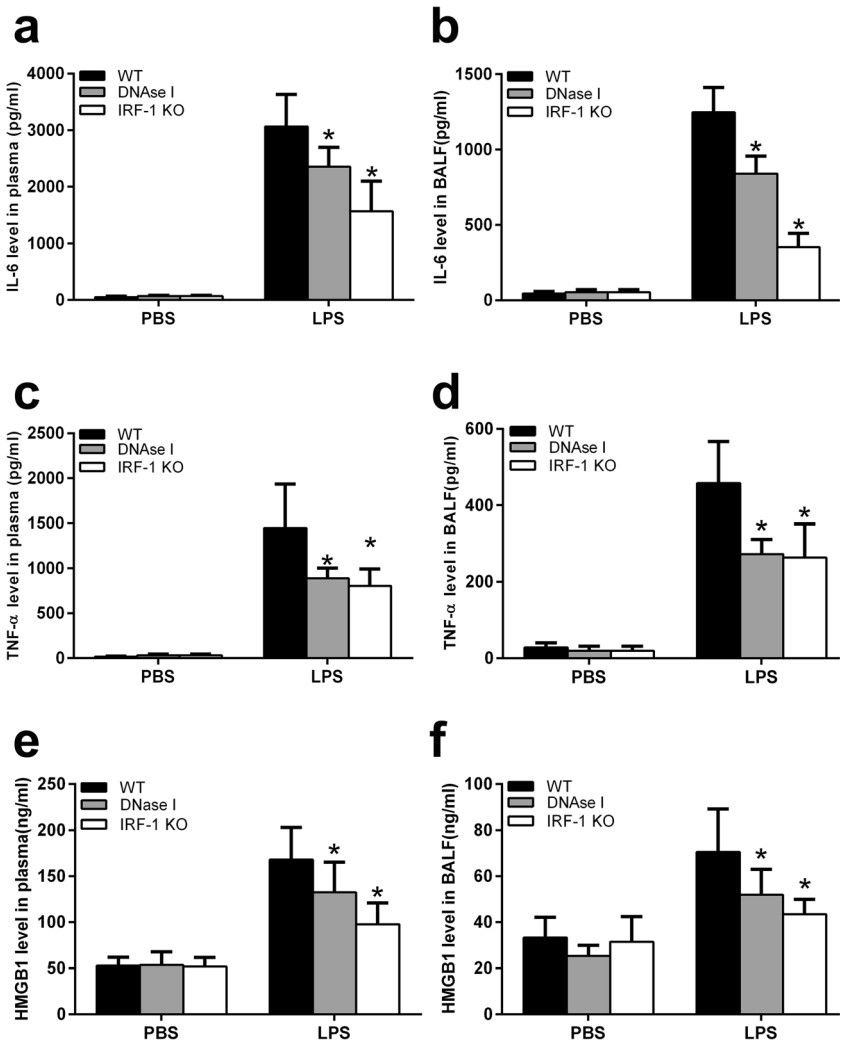

Fig. 4. IRF-1 deletion reduced LPS-induced cytokine levels in mice. WT and IRF-1 KO mice were treated with DNase I (2000 U) at time 0 and 10 h after LPS (5 mg/kg) or PBS injection, and plasma and BALF samples were harvested at 16 h post-treatment and tested for levels of IL-6, TNF-α, and HMGB1 in plasma (**a**, **c**, **e**) and BALF (**b**, **d**, **f**); ($n = 6$/group, $^*P < 0.05$ *vs.* the WT/PBS group). The results are representative of three independent experiments. *IRF-1* interferon regulatory factor 1; *KO* knockout; *WT* wild type; *DNase I* deoxyribonuclease I; *LPS* lipopolysaccharide; *PBS* phosphate-buffered saline; *BALF* bronchoalveolar lavage fluid.

8 h. Western blotting analysis showed that IRF-1 protein levels peaked at 1 h and were weak but detectable at the 10 min time point (Fig. 7a, b).

Next, we used neutrophils of bone marrow from WT and IRF-1 KO mice and stimulated them with LPS-stimulated platelets for 90 min, which represented classical NETosis. The data showed that IRF-1 KO caused decreased NET release, indicated by the reduction of MPO-DNA complexes in the supernatant (Fig. 7c). DHR probes revealed that ROS production induced by LPS-stimulated platelets in neutrophils of IRF-1 KO mice was significantly decreased (Fig. 7d). Then, we further confirmed our findings using western blot analysis and found the same results as shown in Fig. 7c (Fig. 7e, f). Thus, IRF-1 KO inhibits the formation of NETs through ROS *via* classical NETosis.

In contrast to classical NETosis, IRF-1 expression was weak in the period of early/rapid NETosis (Fig. 7a, b). This finding suggests that IRF-1 may not be involved in the early/rapid NETosis mechanism. Our subsequent experiments confirmed this hypothesis: we observed that NETs, based on the co-localization of extracellular DNA with Cit-H3 as well as NE, were formed regardless of

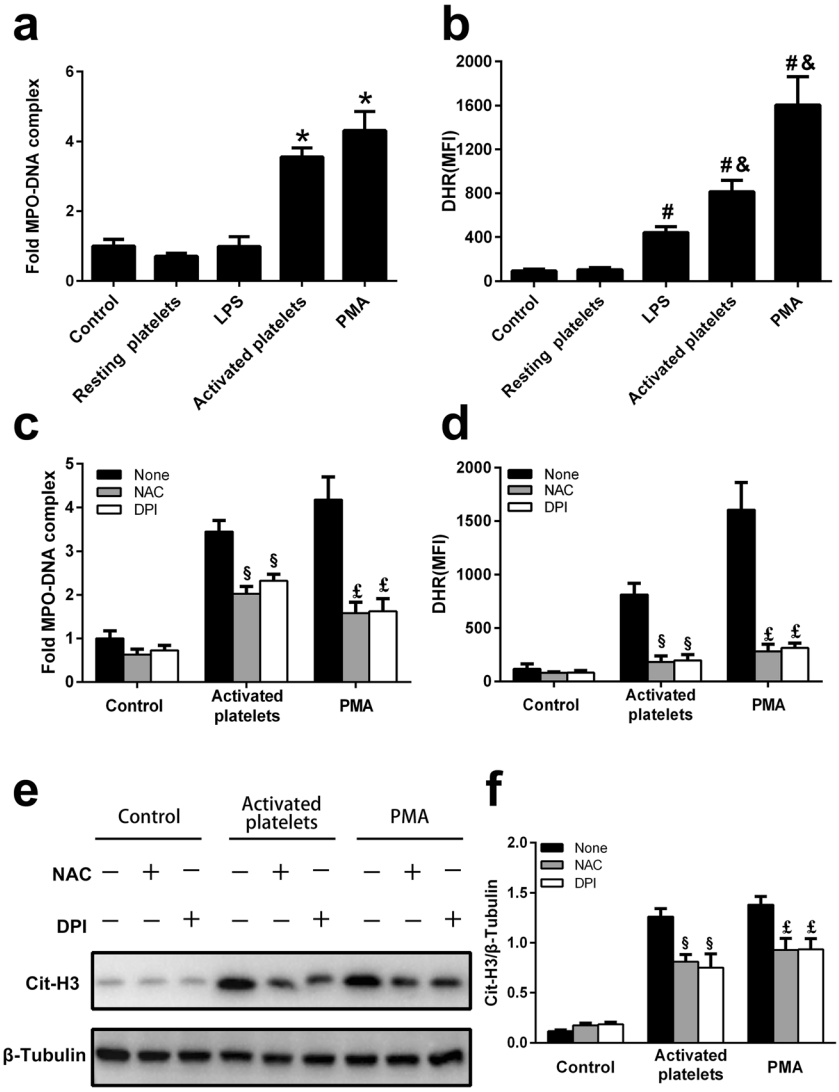

Fig. 5. Production of ROS following LPS-activated platelets leads to classical NETosis. Neutrophils (5×10^5) from bone marrow of WT mice were left untreated or stimulated with 100 nM PMA as negative and positive controls for NET formation, respectively. In addition, neutrophils were co-cultured with resting platelets (5×10^6), LPS (1 μg/ml), and activated platelets for 90 min, followed by measurement of **a** MPO-DNA complex levels in cell supernatants and **b** ROS generation in neutrophils by flow cytometry. In a second set of experiments, neutrophils (5×10^5) were pre-incubated with or without NAC (10 mM) or DPI (10 μM) for 30 min and then treated with nothing, activated platelets (5×10^6) and PMA (100 nM) and incubated with DHR 123 for 90 min to analyze **c** the levels of NETs in supernatants using MPO-DNA capture ELISA assays, **d** the MFI in neutrophils by flow cytometry, and **e**, **f** Cit-H3 protein levels in neutrophils by western blot. $^{*}P < 0.05$ *vs.* the control, resting platelets, and LPS group; $^{\#}P < 0.05$ *vs.* the control and resting platelets group; $^{\&}P < 0.05$ *vs.* the LPS group; $^{\S}P < 0.05$ *vs.* the none/activated platelets group; $^{£}P < 0.05$ *vs.* the none/PMA group; all data shown are representative of at least three separate independent experiments. *WT* wild type; *PMA* phorbol 12-myristate 13-acetate; *LPS* lipopolysaccharide; *NAC* N-acetyl-L-cysteine; *DPI* diphenyleneiodonium; *DHR123* dihydrorhodamine 123; *MFI* mean fluorescence intensity; *Cit-H3* citrullinated histone H3.

whether the neutrophils were from WT or IRF-1 KO mice after a 10-min incubation with LPS-stimulated platelets (Fig. 8a). Additionally, there was no difference in the level of Cit-H3 (Fig. 8b), the quantity of MPO-DNA complexes (Fig. 8c) or ROS production (Fig. 8d) between neutrophils from WT and IRF-KO mice upon a 10-min stimulation with LPS-activated platelets.

In this study, we found that IRF-1 KO attenuates the generation of NETs and ROS production in classical NETosis, but has no effect on the formation of

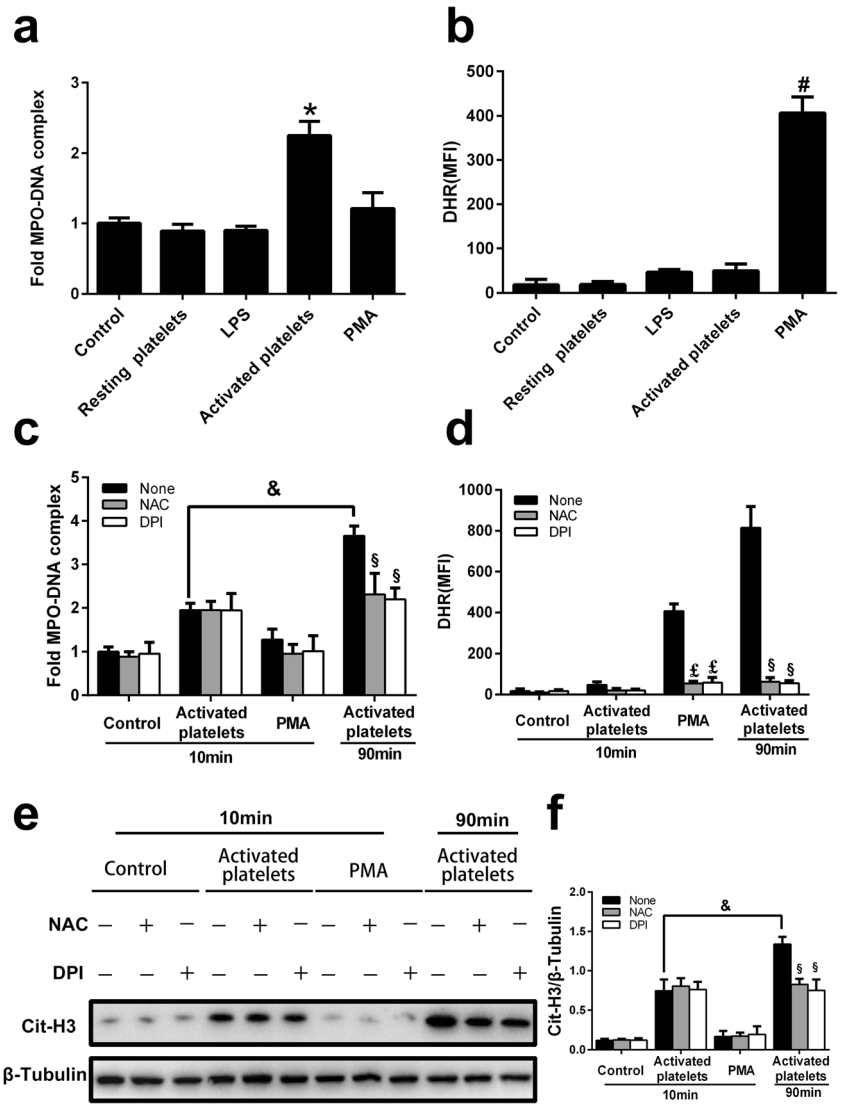

Fig. 6. Early/rapid NETosis mechanism triggered by LPS-stimulated platelets occurs in a ROS-independent manner. Neutrophils (5×10^5) from bone marrow of WT mice were left untreated or stimulated with 100 nM PMA as negative and positive controls for NET formation, respectively. In addition, neutrophils were co-cultured with resting platelets (5×10^6), LPS (1 μg/ml), and activated platelets for 10 min, followed by measurement of **a** MPO-DNA complex levels in cell supernatants and **b** ROS generation in neutrophils by flow cytometry. In a second set of experiments, neutrophils (5×10^5) were pre-incubated with or without NAC (10 mM) or DPI (10 μM) for 30 min and then treated with nothing, activated platelets (5×10^6) and PMA (100 nM) and incubated with DHR 123 for 10 min or 90 min to analyze **c** the levels of MPO-DNA complexes in supernatants, **d** the MFI in neutrophils by flow cytometry, and **e**, **f** Cit-H3 protein levels in neutrophils by western blot. $^{*}P < 0.05$ *vs.* the control, resting platelets, LPS, and PMA group; $^{\#}P < 0.05$ *vs.* the control, resting platelets, LPS, and activated platelets group; $^{\&}P < 0.05$ *vs.* the none/activated platelets group stimulated for 10 min; $^{\S}P < 0.05$ *vs.* the none/activated platelets group stimulated for 90 min; $^{£}P < 0.05$ *vs.* the none/PMA group stimulated for 10 min. All data shown are representative of at least three separate independent experiments. *WT* indicates wild type; *PMA* phorbol 12-myristate 13-acetate; *LPS* lipopolysaccharide; *NAC* N-acetyl-L-cysteine; *DPI* diphenyleneiodonium; *DHR123* dihydrorhodamine 123; *MFI* mean fluorescence intensity; *Cit-H3* citrullinated histone H3.

NETs in the early/rapid NETosis mechanism. Additionally, due to the dominant role of the classical ROS-dependent pathway in the generation of NETs, IRF-1 KO decreased the total levels of NETs *in vitro* after 90 min. However, we hypothesized that excessive NETs formed in classical NETosis were harmful to tissues. The low levels of NETs generated in early/rapid NETosis may play an important role in trapping

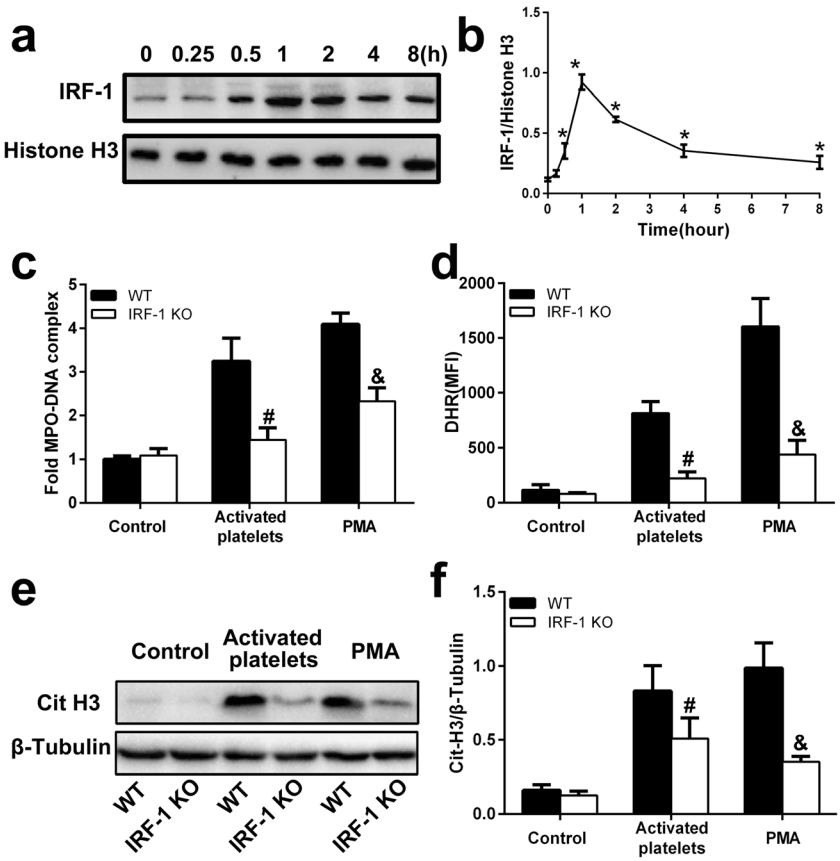

Fig. 7. The kinetic response of IRF-1 to LPS-activated platelets in neutrophils and the role of IRF-1 in regulating NET release through ROS in the classical pathway. **a**, **b** Isolated neutrophils in bone marrow from WT mice were stimulated with activated platelets by LPS for 0, 0.25, 0.5, 1, 2, 4, and 8 h, followed by western blot detection of IRF-1 expression in nuclear extracts from neutrophils. **c** Neutrophils of bone marrow were isolated from WT or IRF-1 KO mice, left untreated, or stimulated with activated platelets or PMA for 90 min. Then, the levels of NETs in supernatants were quantified using MPO-DNA capture ELISA assays, and **d** the generation of ROS in neutrophils, represented by the MFI, was measured by flow cytometry. **e**, **f** Cit-H3 protein levels were determined by western blot in neutrophils treated with activated platelets or PMA for 90 min. $^{*}P < 0.05$ *vs.* the 0 h and 0.25 h group; $^{\#}P < 0.05$ *vs.* the WT/activated platelets group, $^{\&}P < 0.05$ *vs.* the WT/PMA group. All data shown are representative of at least three independent experiments. *IRF-1* interferon regulatory factor 1; *KO* knockout; *WT* wild type; *PMA* phorbol 12-myristate 13-acetate; *MFI* mean fluorescence intensity; *Cit-H3* citrullinated histone H3.

the microorganisms from the infection site or blood and killing them at an early time point. Collectively, these results elucidate why IRF-1 KO decreased the damage caused by NETs in the model of LPS-induced ALI: this change reduces the excessive NETs formed in the classical pathway and retains the protective role of the low levels of NETs generated in the early/rapid NETosis mechanism.

DISCUSSION

ALI/ARDS describe syndromes with diffuse parenchymal lung injury resulting from a variety of inflammatory triggers. Under normal physiological conditions, NETs appear to be an innate immune response that bind microorganisms, prevent them from spreading, and ensure a high local concentration of antimicrobial agents to degrade virulence factors and kill pathogens, thus allowing neutrophils to fulfill their antimicrobial function beyond their life-span. However, accumulating evidence has shown that excessive NET generation results in damaging effects and impaired tissue function during infection-related ALI [9, 31]. Retaining the physiological function of NETs and avoiding the damage caused by excessive NETs may be highly beneficial in designing therapeutic strategies for ALI/ARDS.

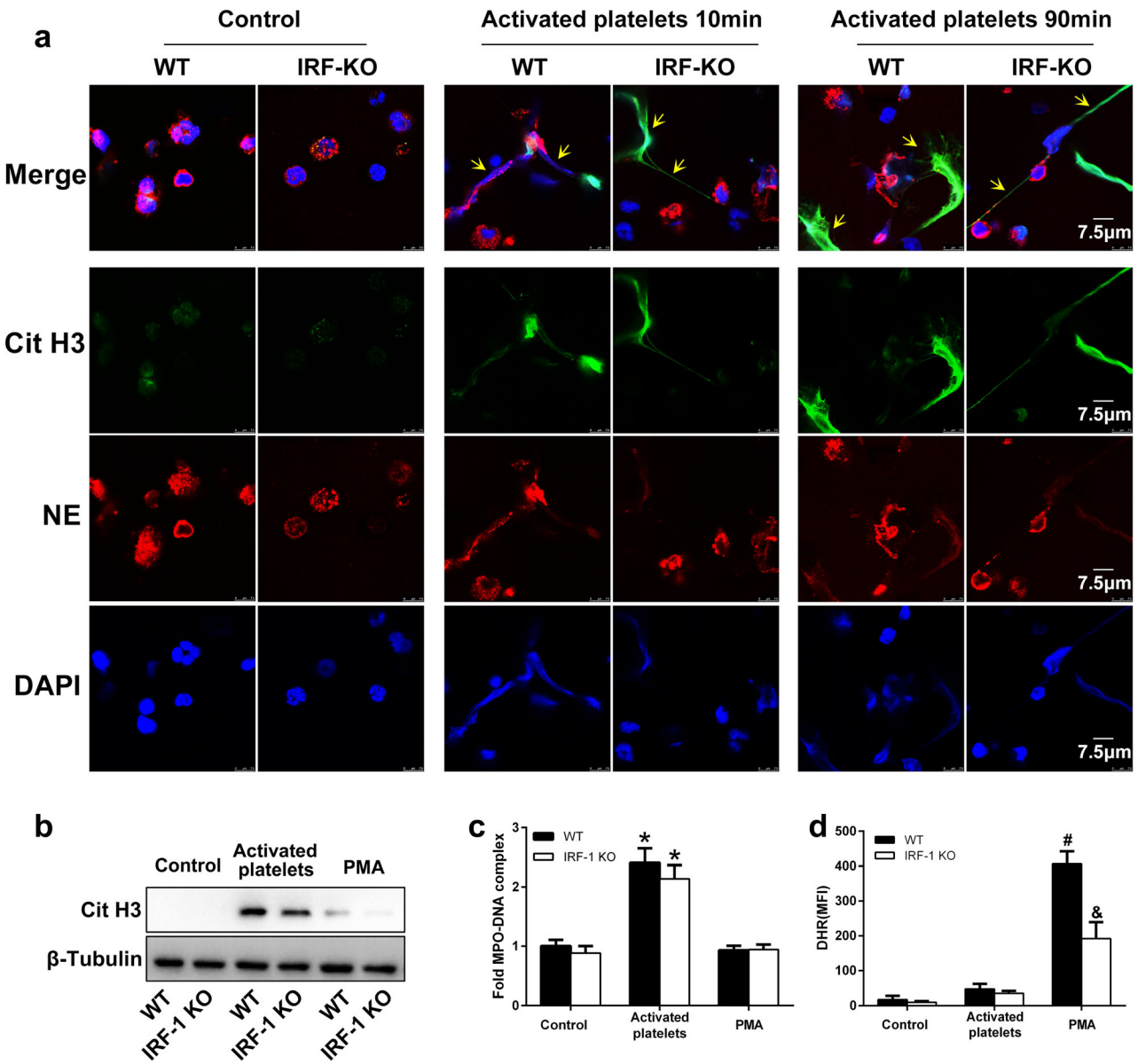

Fig. 8. LPS-activated platelets commit neutrophils to NET generation in early/rapid NETosis in an IRF-1-independent manner. Neutrophils (5×10^5) from bone marrow were isolated from WT or IRF-1 KO mice, left untreated, or stimulated with PMA and activated platelets for 10 min or 90 min. **a** Immunofluorescence staining of NETs was assessed by confocal microscopy in neutrophils. Blue: nuclei; green: Cit-H3; red: NE. **b** Cit-H3 protein levels were determined by western blot in neutrophils treated as described above. **c** The levels of NETs released in supernatants were quantified using MPO-DNA capture ELISA assays. **d** The MFI of neutrophils from WT or IRF-1 KO was analyzed by flow cytometry. $^{*}P < 0.05$ *vs.* the control and PMA group. $^{\#}P < 0.05$ *vs.* the control group and activated platelets group; $^{\&}P < 0.05$ *vs.* WT/PMA group. All data shown are representative of at least three separate independent experiments. *IRF-1* interferon regulatory factor 1; *KO* knockout; *WT* wild type; *PMA* phorbol 12-myristate 13-acetate; *Cit-H3* citrullinated histone H3; *NE* neutrophil elastase; *MFI* mean fluorescence intensity.

In this study, we demonstrated that LPS-triggered NETosis *in vitro* is dependent on the activation of platelets, which is consistent with the work of Clark and his colleagues [25]. Of note, LPS-mediated NETosis *in vivo* is also platelet dependent [22, 26], but the mechanistic link between NET induction and platelet activation *in vivo* and *in vitro* remains unclear. Evidence from the literature indicates that platelet

activation induces thromboxane A2 (TXA2) formation, which triggers the release of platelet factor 4 (PF4) and induces NET release [32]; HMGB1 on the platelet surface or soluble HMGB1 released by activated platelets commits neutrophils to autophagy and NET generation [28, 33]; platelets GPIb, TLR4, and β2 integrin (CD18) on the neutrophil's surface have been shown to be involved in platelet-mediated NETosis in mice and humans [25, 32]. Of note, TXA2 also promotes the release of von Willebrand factor (vWF), a mediator that binds to GPIb in platelets and CD18 in neutrophils and induces platelet-mediated NET formation in humans [32]. In mice, platelet-derived chemokines, such as PF4 (CXCL4) and RANTES (CCL5), act through G protein-coupled receptors (GPCRs) [34]; the interaction between P-selectin-PSGL-1 and integrin $\alpha_{IIb}\beta_3$-Mac-1 is required for the release of NETs in mice [22, 26, 35, 36]. Additionally, activated platelets induce the generation of NETs independently of the platelet stimuli, such as LPS, *S. aureus*, or classic platelet agonists such as ADP [32]. Although the signaling involved in platelet-mediated NET formation is not fully elucidated, the activation of ERK, PI3K, and Src kinases, but not P38, is required for activated platelet-triggered NET release [32, 37]. Notably, whether the NADPH oxidase complex mediated the formation of NETs induced by activated platelets is unclear: Carestia et al. found that blocking the generation of ROS by DPI, an inhibitor of NADPH oxidase, had no effects on the formation of NETs in human neutrophils cells [32]; however, Rossaint and his colleagues observed that pretreatment of mouse neutrophils with DPI significantly decreased NET release *in vitro* and *in vivo* [34]. These results suggest that whether NADPH oxidase contributes to the formation of NETs triggered by activated platelets may be related to the characteristics of human and animal species, and further studies are required to elucidate the signaling pathways involved in platelet-mediated NETosis.

The ROS requirement for NET formation depends on the stimulus, as many studies have reported that ROS generation is essential for NET release, while others have shown them to be dispensable [20, 23, 30]. In this study, we demonstrated that LPS-stimulated platelets induce NET release through two kinetically and mechanistically distinct processes: a ROS-independent early/rapid NETosis, occurring only 10 min. after activated platelets contact, followed by a later ROS-dependent classical NETosis. In the early/rapid NETosis, LPS-stimulated platelets failed to promote the accumulation of ROS. In the later classical NETosis, activated platelets induced by LPS promoted the generation of ROS, which may be because the HMGB1 present in the platelet cell membrane caused TLR4-dependent activation of NADPH oxidase through both the MyD88-IRAK4-p38 MAPK and MyD88-IRAK4-Akt signaling pathways [27, 28]. In addition, NETs released in the supernatant also promoted ROS production when co-cultured with isolated neutrophils of mice [29]. Furthermore, compared with the early/rapid ROS-independent NETosis mechanism, the levels of NETs released in the late classical ROS-dependent pathway were much higher, indicating that the classical ROS-dependent pathway is the dominant mechanism of NET production.

IRF-1 was the first identified member of the IRF family of transcription factors [38]. The initial description of IRF-1 focused on its ability to transcriptionally regulate the expression of type I interferons, but a number of cellular processes, including proliferation, response to tumors and viruses, and immune modulation, have now been shown to be affected by IRF-1 activation [38, 39]. In the present study, we identified the critical role of IRF-1 in mediating lung injury during sepsis-related ALI/ARDS induced by LPS. Indeed, as a gene noted for its involvement in the interferon pathway, IRF-1 is often elevated in ARDS patients [40]. Additionally, disruption of IRF-1 in the mouse model alleviated lung injury and protected against LPS insult. Furthermore, IRF-1 may also control the release of inflammatory mediators. The present study demonstrated that IL-6, TNF-α, and HMGB1 are significantly reduced both in plasma and BALF in IRF-1 KO mice during LPS-induced acute lung injury. Interestingly, treatment with DNase I had similar effects, which indicates that IRF-1 could play a key role in NETosis-associated cytokines. These studies indicate that IRF-1 plays an important role in mediating lung injury and inflammatory response in ALI/ARDS.

In this study, we demonstrated that IRF-1 can regulate the formation of NETs in classical NETosis. We found that IRF-1 KO attenuates the generation of ROS production in neutrophils, which resulted in the intervention of classical NETosis stimulated by LPS *in vivo* and LPS-stimulated platelets after 90 min *in vitro*. Previous studies have confirmed the importance of IRF-1 in ROS production, primarily by regulating mitochondrial function [16, 41]; notably, mitochondrial ROS are necessary for NET formation [42]. However, IRF-1 also mediates the release of

inflammatory mediators, such HMGB1, TNF-α, and IL-1β [14, 18], which also contribute to the accumulation of ROS. However, a limitation of this study is that we only evaluated the role of IRF-1 in determining the total ROS in neutrophils and the effects of IRF-1 on regulating different sources of ROS, including NADPH oxidase, mitochondrial ROS, xanthine oxidase (XO), uncoupling of nitric oxide synthase (NOS), and cytochrome P450, remain unexplained and will be investigated in our subsequent experiments.

In contrast to classical NETosis, IRF-1 was not involved in the early/rapid NETosis, as there was no difference in the quantity of NETs between neutrophils from WT and IRF-1 KO mice after 10-min incubation with LPS-stimulated platelets. One possible reason for this is that the active functional form of IRF-1 may not exert its activity in such a short time period. Alternatively, activated platelets may be unable to induce sufficient ROS to commit neutrophils to form NETs. Additionally, it is worth noting that the excess NETs formed in classical NETosis are harmful to tissues; however, the low levels of NETs generated in early/rapid NETosis may play an important role in trapping the microorganisms from the infection site or blood and killing them at an early time point.

In conclusion, we demonstrated that NETs can be induced by LPS-stimulated platelets in neutrophils through both an early/rapid ROS-independent and classical ROS-dependent pathway. A better understanding of the two mechanisms of NET release and the effects of NETs on the host immune system modulation, including addressing the role of IRF-1 in modulating ROS production, retaining the physiological function of NETs, and avoiding the damage caused by excessive NETs formed in the classical mechanism, could support the development of new potential therapeutic strategies for ALI/ARDS.

AUTHOR CONTRIBUTIONS

S.L. performed the experiments and drafted the manuscript; S.L., Y.Y., Y.L., Z.M., and H.L. analyzed the data; S.L. and X.S. interpreted the experimental results; L.Z. verified the pathological results; S.L., H.L., Q.L., and M.D. prepared the figures; P.P. conceived and designed the research; P.P. and L.Z. edited and revised the manuscript; P.P. approved the final version of manuscript. All authors read and approved the final manuscript.

FUNDING INFORMATION

This work was supported by the National Natural Science Foundation of China (nos. 81770080 and 81470266).

COMPLIANCE WITH ETHICAL STANDARDS

Conflict of Interest. The authors declare no competing interests.

REFERENCES

1. Matthay, M.A., L.B. Ware, and G.A. Zimmerman. 2012. The acute respiratory distress syndrome. *The Journal of Clinical Investigation* 122 (8): 2731–2740.
2. Modrykamien, A.M., and P. Gupta. 2015. The acute respiratory distress syndrome. *Proceedings (Baylor University Medical Center)* 28 (2): 163–171.
3. Bellani, G., J.G. Laffey, T. Pham, E. Fan, L. Brochard, A. Esteban, L. Gattinoni, F. Van Haren, A. Larsson, and D.F. Mcauley. 2016. Epidemiology, patterns of care, and mortality for patients with acute respiratory distress syndrome in intensive care units in 50 countries. *JAMA* 315 (8): 788–800.
4. Matute-Bello, G., C.W. Frevert, and T.R. Martin. 2008. Animal models of acute lung injury. *American Journal of Physiology. Lung Cellular and Molecular Physiology* 295 (3): L379–L399.
5. Chen, H., C. Bai, and X. Wang. 2010. The value of the lipopolysaccharide-induced acute lung injury model in respiratory medicine. *Expert Review of Respiratory Medicine* 4 (6): 773–783.
6. Perl, M., J. Lomas-Neira, F. Venet, C.S. Chung, and A. Ayala. 2011. Pathogenesis of indirect (secondary) acute lung injury. *Expert Review of Respiratory Medicine* 5 (1): 115–126.
7. Welbourn, C.R., and Y. Young. 1992. Endotoxin, septic shock and acute lung injury: Neutrophils, macrophages and inflammatory mediators. *The British Journal of Surgery* 79 (10): 998–1003.
8. Brinkmann, V., U. Reichard, C. Goosmann, B. Fauler, Y. Uhlemann, D.S. Weiss, Y. Weinrauch, and A. Zychlinsky. 2004. Neutrophil extracellular traps kill bacteria. *Science* 303 (5663): 1532–1535.
9. Liu, S., X. Su, P. Pan, L. Zhang, Y. Hu, H. Tan, D. Wu, et al. 2016. Neutrophil extracellular traps are indirectly triggered by lipopolysaccharide and contribute to acute lung injury. *Scientific Reports* 6: 37252.
10. Fuchs, T.A., U. Abed, C. Goosmann, R. Hurwitz, I. Schulze, V. Wahn, Y. Weinrauch, V. Brinkmann, and A. Zychlinsky. 2007. Novel cell death program leads to neutrophil extracellular traps. *The Journal of Cell Biology* 176 (2): 231–241.
11. Pilsczek, F.H., D. Salina, K.K. Poon, C. Fahey, B.G. Yipp, C.D. Sibley, S.M. Robbins, et al. 2010. A novel mechanism of rapid nuclear neutrophil extracellular trap formation in response to Staphylococcus aureus. *Journal of Immunology* 185 (12): 7413–7425.
12. Zhang, L., J.S. Cardinal, P. Pan, B.R. Rosborough, Y. Chang, W. Yan, H. Huang, T.R. Billiar, M.R. Rosengart, and A. Tsung. 2012.

Splenocyte apoptosis and autophagy is mediated by interferon regulatory factor 1 during murine endotoxemia. *Shock* 37 (5): 511–517.
13. Zhang, L., J.S. Cardinal, R. Bahar, J. Evankovich, H. Huang, G. Nace, T.R. Billiar, M.R. Rosengart, P. Pan, and A. Tsung. 2012. Interferon regulatory factor-1 regulates the autophagic response in LPS-stimulated macrophages through nitric oxide. *Molecular Medicine* 18: 201–208.
14. Pan, P.H., J. Cardinal, M.L. Li, C.P. Hu, and A. Tsung. 2013. Interferon regulatory factor-1 mediates the release of high mobility group box-1 in endotoxemia in mice. *Chinese Medical Journal* 126 (5): 918–924.
15. Huang, H., S. Tohme, A.B. Al-Khafaji, S. Tai, P. Loughran, L. Chen, S. Wang, et al. 2015. Damage-associated molecular pattern-activated neutrophil extracellular trap exacerbates sterile inflammatory liver injury. *Hepatology* 62 (2): 600–614.
16. Lee, H.J., Y.K. Oh, M. Rhee, J.Y. Lim, J.Y. Hwang, Y.S. Park, Y. Kwon, K.H. Choi, I. Jo, S.I. Park, B. Gao, and W.H. Kim. 2007. The role of STAT1/IRF-1 on synergistic ROS production and loss of mitochondrial transmembrane potential during hepatic cell death induced by LPS/d-GalN. *Journal of Molecular Biology* 369 (4): 967–984.
17. Remijsen, Q., Berghe T. Vanden, E. Wirawan, B. Asselbergh, E. Parthoens, R. De Rycke, S. Noppen, M. Delforge, J. Willems, and P. Vandenabeele. 2011. Neutrophil extracellular trap cell death requires both autophagy and superoxide generation. *Cell Research* 21 (2): 290–304.
18. Wu, D., P. Pan, X. Su, L. Zhang, Q. Qin, H. Tan, L. Huang, and Y. Li. 2016. Interferon regulatory Factor-1 mediates alveolar macrophage pyroptosis during LPS-induced acute lung injury in mice. *Shock* 46 (3): 329–338.
19. Liu, D.D., S.J. Kao, and H.I. Chen. 2008. N-acetylcysteine attenuates acute lung injury induced by fat embolism. *Critical Care Medicine* 36 (2): 565–571.
20. Barth, C.R., G.A. Funchal, C. Luft, J.R. de Oliveira, B.N. Porto, and M.V. Donadio. 2016. Carrageenan-induced inflammation promotes ROS generation and neutrophil extracellular trap formation in a mouse model of peritonitis. *European Journal of Immunology* 46 (4): 964–970.
21. McGuigan, R.M., P. Mullenix, L.L. Norlund, D. Ward, M. Walts, and K. Azarow. 2003. Acute lung injury using oleic acid in the laboratory rat: Establishment of a working model and evidence against free radicals in the acute phase. *Current Surgery* 60 (4): 412–417.
22. Caudrillier, A., K. Kessenbrock, B.M. Gilliss, J.X. Nguyen, M.B. Marques, M. Monestier, P. Toy, Z. Werb, and M.R. Looney. 2012. Platelets induce neutrophil extracellular traps in transfusion-related acute lung injury. *The Journal of Clinical Investigation* 122 (7): 2661–2671.
23. Parker, H., M. Dragunow, M.B. Hampton, A.J. Kettle, and C.C. Winterbourn. 2012. Requirements for NADPH oxidase and myeloperoxidase in neutrophil extracellular trap formation differ depending on the stimulus. *Journal of Leukocyte Biology* 92 (4): 841–849.
24. Pieterse, E., N. Rother, C. Yanginlar, L.B. Hilbrands, and J. van der Vlag. 2016. Neutrophils discriminate between lipopolysaccharides of different bacterial sources and selectively release neutrophil extracellular traps. *Frontiers in Immunology* 7: 484.
25. Clark, S.R., A.C. Ma, S.A. Tavener, B. McDonald, Z. Goodarzi, M.M. Kelly, K.D. Patel, S. Chakrabarti, E. McAvoy, G.D. Sinclair, E.M. Keys, E. Allen-Vercoe, R. DeVinney, C.J. Doig, F.H.Y. Green, and P. Kubes. 2007. Platelet TLR4 activates neutrophil extracellular traps to ensnare bacteria in septic blood. *Nature Medicine* 13 (4): 463–469.
26. McDonald, B., R. Urrutia, B.G. Yipp, C.N. Jenne, and P. Kubes. 2012. Intravascular neutrophil extracellular traps capture bacteria from the bloodstream during sepsis. *Cell Host & Microbe* 12 (3): 324–333.
27. Fan, J., Y. Li, R.M. Levy, J.J. Fan, D.J. Hackam, Y. Vodovotz, H. Yang, K.J. Tracey, T.R. Billiar, and M.A. Wilson. 2007. Hemorrhagic shock induces NAD (P) H oxidase activation in neutrophils: Role of HMGB1-TLR4 signaling. *Journal of Immunology* 178 (10): 6573–6580.
28. Maugeri, N., L. Campana, M. Gavina, C. Covino, M. De Metrio, C. Panciroli, L. Maiuri, et al. 2014. Activated platelets present high mobility group box 1 to neutrophils, inducing autophagy and promoting the extrusion of neutrophil extracellular traps. *Journal of Thrombosis and Haemostasis* 12 (12): 2074–2088.
29. Merza, M., H. Hartman, M. Rahman, R. Hwaiz, E. Zhang, E. Renstrom, L. Luo, M. Morgelin, S. Regner, and H. Thorlacius. 2015. Neutrophil extracellular traps induce trypsin activation, inflammation, and tissue damage in mice with severe acute pancreatitis. *Gastroenterology* 149 (7): 1920–1931.e1928.
30. Rochael, N.C., A.B. Guimaraes-Costa, M.T. Nascimento, T.S. DeSouza-Vieira, M.P. Oliveira, E. Souza LF Garcia, M.F. Oliveira, and E.M. Saraiva. 2015. Classical ROS-dependent and early/rapid ROS-independent release of neutrophil extracellular traps triggered by Leishmania parasites. *Scientific Reports* 5: 18302.
31. Saffarzadeh, M., C. Juenemann, M.A. Queisser, G. Lochnit, G. Barreto, S.P. Galuska, J. Lohmeyer, and K.T. Preissner. 2012. Neutrophil extracellular traps directly induce epithelial and endothelial cell death: A predominant role of histones. *PLoS One* 7 (2): e32366.
32. Carestia, A., T. Kaufman, L. Rivadeneyra, V.I. Landoni, R.G. Pozner, S. Negrotto, L.P. D'Atri, R.M. Gomez, and M. Schattner. 2016. Mediators and molecular pathways involved in the regulation of neutrophil extracellular trap formation mediated by activated platelets. *Journal of Leukocyte Biology* 99 (1): 153–162.
33. Tadie, J.M., H.B. Bae, S. Jiang, D.W. Park, C.P. Bell, H. Yang, J.F. Pittet, K. Tracey, V.J. Thannickal, and E. Abraham. 2013. HMGB1 promotes neutrophil extracellular trap formation through interactions with toll-like receptor 4. *American Journal of Physiology Lung Cellular and Molecular Physiology* 304 (5): L342–L349.
34. Rossaint, J., J.M. Herter, H. Van Aken, M. Napirei, Y. Doring, C. Weber, O. Soehnlein, and A. Zarbock. 2014. Synchronized integrin engagement and chemokine activation is crucial in neutrophil extracellular trap-mediated sterile inflammation. *Blood* 123 (16): 2573–2584.
35. Etulain, J., K. Martinod, S.L. Wong, S.M. Cifuni, M. Schattner, and D.D. Wagner. 2015. P-selectin promotes neutrophil extracellular trap formation in mice. *Blood* 126 (2): 242–246.
36. Sreeramkumar, Vinatha, José M. Adrover, Ivan Ballesteros, Maria Isabel Cuartero, Jan Rossaint, Izaskun Bilbao, Maria Nácher, Christophe Pitaval, Irena Radovanovic, and Yoshinori Fukui. 2014. Neutrophils scan for activated platelets to initiate inflammation. *Science* 346 (6214): 1234–1238.
37. Carestia, A., T. Kaufman, and M. Schattner. 2016. Platelets: New bricks in the building of neutrophil extracellular traps. *Frontiers in Immunology* 7: 271.
38. Kroger, A., M. Koster, K. Schroeder, H. Hauser, and P.P. Mueller. 2002. Activities of IRF-1. *Journal of Interferon & Cytokine Research* 22 (1): 5–14.
39. Fujita, T., J. Sakakibara, Y. Sudo, M. Miyamoto, Y. Kimura, and T. Taniguchi. 1988. Evidence for a nuclear factor(s), IRF-1, mediating induction and silencing properties to human IFN-beta gene regulatory elements. *The EMBO Journal* 7 (11): 3397–3405.
40. Baas, T., J.K. Taubenberger, P.Y. Chong, P. Chui, and M.G. Katze. 2006. SARS-CoV virus-host interactions and comparative etiologies

of acute respiratory distress syndrome as determined by transcriptional and cytokine profiling of formalin-fixed paraffin-embedded tissues. *Journal of Interferon & Cytokine Research* 26 (5): 309–317.

41. Gao, J., M. Senthil, B. Ren, J. Yan, Q. Xing, J. Yu, L. Zhang, and J.H. Yim. 2010. IRF-1 transcriptionally upregulates PUMA, which mediates the mitochondrial apoptotic pathway in IRF-1-induced apoptosis in cancer cells. *Cell Death and Differentiation* 17 (4): 699–709.

42. Lood, C., L.P. Blanco, M.M. Purmalek, C. Carmona-Rivera, S.S. De Ravin, C.K. Smith, H.L. Malech, J.A. Ledbetter, K.B. Elkon, and M.J. Kaplan. 2016. Neutrophil extracellular traps enriched in oxidized mitochondrial DNA are interferogenic and contribute to lupus-like disease. *Nature Medicine* 22 (2): 146–153.